



**HAL**  
open science

## Study of the interactions between a water spray and a moving layer of hot smoke

Louis Hardy, Anthony Collin, Mathieu Suzanne, Giacomo Erez, Rabah Mehaddi, Pascal Boulet

### ► To cite this version:

Louis Hardy, Anthony Collin, Mathieu Suzanne, Giacomo Erez, Rabah Mehaddi, et al.. Study of the interactions between a water spray and a moving layer of hot smoke. 2023. hal-04199488

**HAL Id: hal-04199488**

**<https://hal.univ-lorraine.fr/hal-04199488>**

Preprint submitted on 7 Sep 2023

**HAL** is a multi-disciplinary open access archive for the deposit and dissemination of scientific research documents, whether they are published or not. The documents may come from teaching and research institutions in France or abroad, or from public or private research centers.

L'archive ouverte pluridisciplinaire **HAL**, est destinée au dépôt et à la diffusion de documents scientifiques de niveau recherche, publiés ou non, émanant des établissements d'enseignement et de recherche français ou étrangers, des laboratoires publics ou privés.



Distributed under a Creative Commons Attribution 4.0 International License

# Study of the interactions between a water spray and a moving layer of hot smoke

L. Hardy<sup>a,b</sup>, A. Collin<sup>b,1</sup>, M. Suzanne<sup>a</sup>, G. Erez<sup>a</sup>, R. Mehaddi<sup>b</sup> and P. Boulet<sup>b</sup>

*a*: LCPP, Préfecture de Police de Paris, F-75015 Paris, France

*b*: Université de Lorraine, CNRS, LEMTA, F-54000 Nancy, France

Keywords: smoke propagation, water spray, cooling effect, model scale tests

## Abstract

This study compares the effects on a smoke layer of water sprays injected downward, upward or according to an inclined counter-flow configuration. The impact is analyzed considering stratification, mixing and cooling effects upstream (fire side) and downstream (opening side) the position of the spray. The experiments were conducted in a  $1/5^{th}$  scale model reproducing a room connected to a corridor. The injection of the poly-dispersed spray was carried out in the corridor where a layer of smoke was flowing in the upper part. Thanks to the experimental configuration, there is no direct impact of the spray on the fire source and the production of smoke, but only on the hot flow of smoke. The effect of the spray was evaluated for the different directions of injection and two water feeding pressures. The measurement have shown that effective cooling of the upper layer is observed downstream of the spray. The efficiency of the cooling is dependent on the injection angle. A more or less significant heating of the lower layer is measured upstream for all the injection angles. The injection angle has an influence on the smoke mixing and cooling, an upward spray injection is more efficient. The strongest interaction is observed for an inclined counter-flow injection, similar to the configuration of firefighters cooling a smoke layer while moving forward in a corridor toward a fire source. Moreover, two water injection pressures were investigated: 4 and 8 bars. Increasing this pressure reduces the droplet diameter and increases the water flow rate. In the present experimental configuration, modifying the water injection pressure does not change the observations made. All experimental data are available in an open-access database for

---

<sup>1</sup>Corresponding author: anthony.collin@univ-lorraine.fr

further uses.

## Introduction

Smoke control during firefighting operations is essential to maintain safety conditions for occupants and firefighters and to limit the fire development. Several operational devices may be used to control a smoke layer, including mechanical or natural ventilation, or the use of solid curtain (fabric curtain for instance). However, it is important to differentiate fire safety studies dedicated to smoke extraction for example, from studies focused on firefighter's concerns. Indeed, the main hazard for firefighters does not lie on the toxicity of the smoke thanks to the use of insulating breathing apparatus, but rather on the temperature and the flammable nature of the smoke layer or the radiation coming from the smoke layer. It is therefore necessary to efficiently cool the upper smoke layer while preserving the lower part of the corridor to keep good visibility conditions.

In a fire situation, the application of water can be produced by different devices such as a water mist system, a water sprinkler or a hose nozzle. The effects and goals of these devices can be different and impact the fire development by different aspects. The first effect is a momentum exchange. During the water spray application, the momentum lost by droplets is transferred to the air flow by drag effect and air will therefore move in the same direction as droplets. This interaction can partially block the smoke propagation in confined situations as recently demonstrated by Sun *et al.* [1] or Mehaddi *et al.* [2].

Moreover, water spray curtains have been studied as possible solutions for providing a shielding effect against radiation (see the numerical and experimental studies by Parent *et al.* [3] and Collin *et al.* [4] for example). In these configurations, the aim is to protect given devices, goods or people from strong radiations, due to flames. This is achieved thanks to a combination of absorption and scattering of radiation by water droplets.

Numerous studies have been conducted to quantify the effects of various fire safety systems, sprinklers or water curtains. Most studies focused on the impact of a downward spray, in a stationary or mobile smoke layer based on experimental or numerical studies [5, 6, 7, 8, 9, 10, 11, 2]. As expected, these studies show a destratification of the smoke layer due to a cooling effect and also to momentum exchange with the spray which drags the smoke downwards, as demonstrated by Bullen [5] and more recently recalled by Tang *et al.* [9].

However, to our best knowledge, no study could be found regarding the behavior of smoke during the application of an upward or inclined spray inside a corridor, which corresponds to the actions of hose nozzles that firefighters can carry out during their operations.

The main objective of this contribution is therefore to characterize the impact of the actions that firefighters can have on the smoke flow when activating their nozzle and find which spray parameters are the most influential on the stratification and the cooling of smoke.

The experimental setup used in this study is the  $1/5^{th}$  scale model of the configuration studied by Morlon *et al.* [12] and Blanchard *et al.* [13], designed as a main room where a pool fire is developed, connected to an adjacent corridor. In [12], the authors compared the thermal and optical vertical profiles measured in the smoke layer during and after water mist applications. They characterized the smoke flow by thermal devices (thermocouples) and opacimeters. In [13], the authors tested three water sprays located inside the corridor (one high-pressure water mist system and two sprinkler systems for different operating pressures). They analyzed the temperature and transmittance profiles and studied the thermal stratification and the visibility in the corridor. The authors demonstrated that, for the water mist system and the highest-pressure sprinkler system, the smoke cooling is efficient and the visibility is altered, with a loss of stratification in the corridor. On the contrary, with the lowest-pressure sprinkler system, the spray only affected the smoke under the spray.

In a more recent study and using the same configuration as in Blanchard *et al.* [13], Mehaddi *et al.* [14] analyzed the smoke filling of the corridor in a  $1/5^{th}$  scale model. The authors tried to correlate the smoke layer thickness, its mean temperature and its mean velocity to the geometrical characteristics of the corridor and to the Heat Release Rate (*HRR*). They showed that the temperature and velocity profiles are unique when they are scaled using the *HRR*, and that the smoke thickness does not depend on the Heat Release Rate.

The present article will use the same reduced scale experimental setup studied by Mehaddi *et al.* [14] and will also focus on the interactions between a spray and a layer of smoke in a corridor. The impact of the spray activation on the smoke flow will be analyzed in various conditions. A special care will be paid to define the effects of the spray injection orientation and of the droplet size distribution. Experiments will be based on the measurements of the temperature profiles. The originality of the contribution is to propose experimental results for a counter-flow and

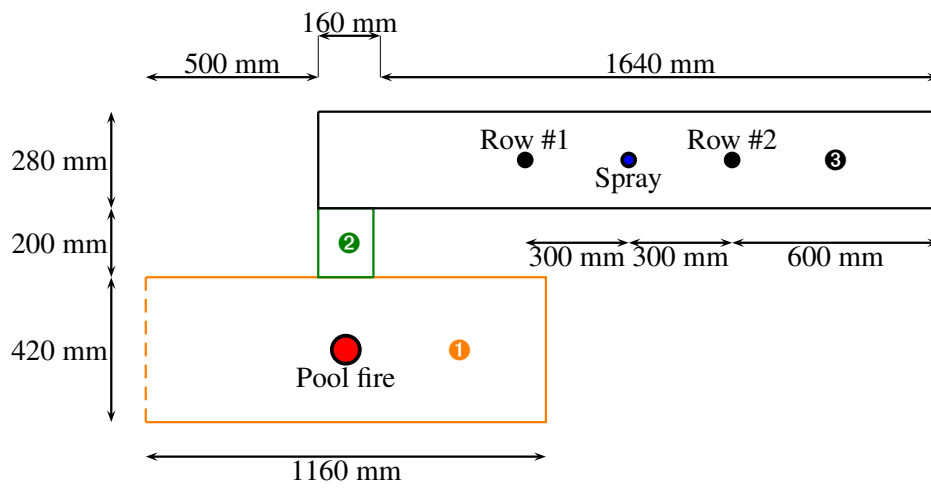
inclined spray ( $45^\circ$ ) or a vertical spray injected upward in the smoke layer. Comparisons will be done with downward injection conditions.

The article is organized as follows: in section 1, the experimental set-up is described and the metrology used is presented. In section 2, the experimental results are discussed. Section 3 will generalize the study with a dimensionless analysis of the interactions between the spray and the smoke layer. Finally, main conclusions will be given in section 4.

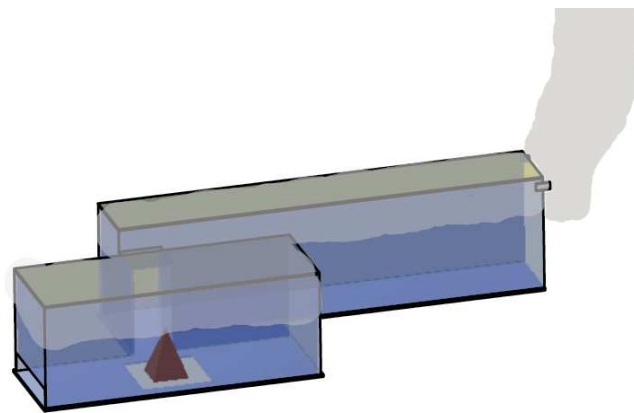
## **1 Experimental setup and conditions**

### **1.1 Geometry description**

The experimental setup was built to study the interactions between a spray and a layer of moving smoke. It is composed of 3 parts, all made of polycarbonate, 5 mm thick, as shown in Figure 1(a). The physical and thermal properties for polycarbonate used can be found in [2]. Zone #1 is the fire zone with a height of 440 mm, a length of 1160 mm and a width of 420 mm. Walls in this area have been reinforced from the inside with a thermal insulation (10 mm thick Fermacell plate) to protect the walls (in Zone #1 and #2 for all walls). In addition, the air intake has been enlarged to allow a better oxygen supply to the fire compared to [14]. Now, the air is supplied in the lower part and along entire width of the rear face of the fire room, as shown by the dotted line in Figure 1(a). The height of this opening is about 80 mm. Zone #2 is an intermediate corridor which allows communication between the fire room and the corridor. This area, also reinforced with insulation, has the following dimensions: length 200 mm, height 380 mm and width 160 mm. Zone #3 is the corridor which is the main focus of this study. The dimensions of this area are a length of 1800 mm, a height of 480 mm and a width of 280 mm. In this corridor, only the part close to the intermediate corridor has been reinforced with insulation (280 mm x 480 mm x 10 mm). An overview of the experimental setup is given in Figure 1(b): the flame is symbolized with a red pyramid shape in the room and the smoke layer is also represented, with the exit flow at the corridor end.



(a) Sketch-up of the experimental setup with the location of the sensors



(b) Overview of the experimental installation during a fire test

Figure 1: Description and dimensions of the experimental setup used in this study

## 1.2 Smoke layer characterization with temperature profiles

Two rows of 24 T-type thermocouples with a 0.2 mm diameter are fixed in the corridor (Zone #3) at 1200 mm and 600 mm from the exit. They are respectively called Row #1 and Row #2 and depicted in Figure 1(a). The distance between each thermocouple is 20 mm (the first one set at 10 mm from the floor, the second at 30 mm, . . . up to the last at 470 mm) allowing to track accurately the vertical position of the interface between the smoke layer and the fresh air in the corridor. These thermocouples are linked to a cDAQ data acquisition system from National Instrument with a time step for the recording set to 1.146 s (minimal value imposed by the data recording system).

## 1.3 Heat Release Rate (HRR) measurements

The pool fire takes place in a 90 mm circular steel pan filled with heptane, located in Zone #1 shown in Figure 1(a). Mass loss monitoring is provided by an electronic weight cell (EXPLORER 10200GX0.01G EX10202 from OHAUS) with an accuracy of 0.01 g. The time step for the acquisition is set at 1 s. The heat release rate is then obtained by estimating,

$$HRR = -\frac{dm}{dt} \times \Delta h_c \quad (1)$$

with  $m$  the mass in g,  $\Delta h_c$  the heat of combustion of heptane in kJ/g and  $HRR$  the heat release rate in kW. The value of the heat of combustion was found in [15] and set to 44.6 kJ/g (a value obtained from experiments which include the efficiency of combustion). The fuel mass was measured continuously during experiments. The raw data were then averaged using a 13 points sliding centered Gaussian window to filter out measurement noise.

These  $HRR$  profiles should be considered as approximate values. In fact, the proposed configuration leads to a fire that is probably under-ventilated and the actual combustion efficiency is unknown. Beside this estimate, the experimental data of the mass loss are available in a database, so that any interested reader may perform his own estimation of the  $HRR$  with a refined model accounting for a deviation from a well-ventilated regime.

## 1.4 Characteristics of water sprays

The chosen injection nozzle is a TP400067 from Spraying Systems & Co. already used in previous studies [14, 16, 17]. This nozzle produces a full elliptic spray of polydispersed droplets. The size distribution of the droplets may be

Pressure	Flow rate	Spray cone	$D_{10}$	$D_{20}$	$D_{30}$	$D_{32}$	$\mu$	$\sigma$
[bar]	[L/min]	angle [°]	[ $\mu\text{m}$ ]	[ $\mu\text{m}$ ]	[ $\mu\text{m}$ ]	[ $\mu\text{m}$ ]	[ $\mu\text{m}$ ]	[–]
4	0.32	18 and 45	173	186	198	226	157	0.399
8	0.40	21 and 55	155	165	177	202	146	0.367

Table 1: Nozzle supply parameters and their characteristics

modified in adjusting the nozzle water supply pressure. Two pressures were considered in this work, 4 and 8 bars. Note that other techniques (not considered here), such as the addition of surfactants, also aim at controlling the droplet size by modifying their interfacial properties [18, 19].

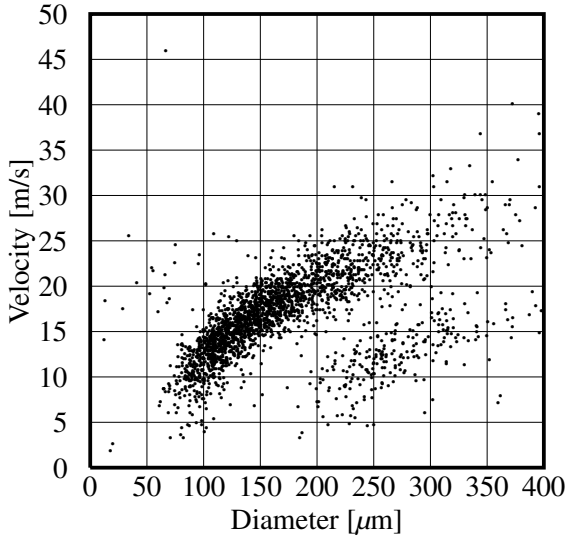
The orifice diameter of the nozzle is about 0.53 mm and the flow rate number (or the so-called discharge coefficient or K-Factor) is  $8.5 \cdot 10^{-9} \text{ m}^3/\text{s}/\text{Pa}^{1/2}$ . All the features of this nozzle regarding the operating pressure are summed up in Table 1 and are characterized when the spray is in a downward position. Since the spray patterns are elliptical, two spray cone angles are defined for each pressure. The spray nozzle has been set to insure that the major axis of the spray pattern follows the corridor width.

The measurements of the average diameters were carried out using a Sprayspy apparatus (Time Shift Measurement System), from AOM System. This experimental device measure spatially resolved single droplet events and allows to measure the distributions of the droplet diameters and velocity [20, 21] thanks to an innovative optical measurement technique. This spray characterization is done 20 cm below the nozzle outlet along the central axis in a downward spray configuration.

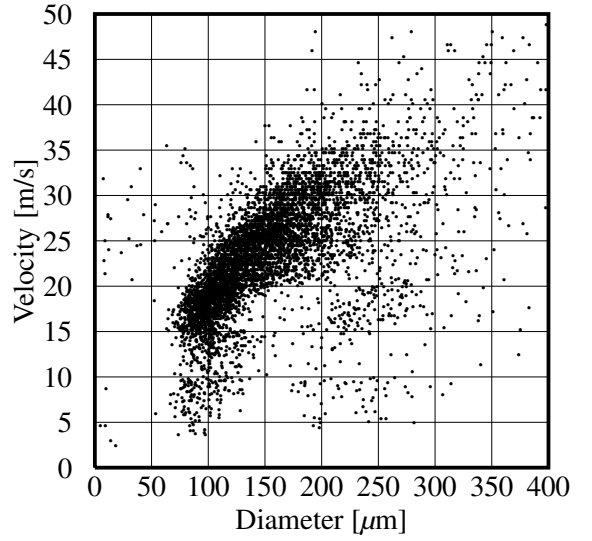
Figure 2 gives, for each tracked droplets, the velocity versus the corresponding droplet diameter for two supply pressures of 4 and 8 bars. For both pressures, the droplet diameters range from 75 to 400  $\mu\text{m}$ , and the velocities vary between 5 and 50 m/s.

Table 1 gives the mean diameters estimated for TP400067 at 4 and 8 bars. These mean diameters are evaluated based





(a) 4 bars, measurements on 2321 droplets



(b) 8 bars, measurements on 5480 droplets

Figure 2: Velocity/Diameter distributions of TP400067 waterspray at 20 cm below the injection point for different operating pressures

on the following relationship,

$$D_{pq}^{p-q} = \frac{\sum_{i=1}^{N_{\text{droplets}}} D_i^p}{\sum_{i=1}^{N_{\text{droplets}}} D_i^q} \quad (2)$$

where  $N_{\text{droplets}}$  is the total number of droplets caught-up by the SpraySpy apparatus.  $p$  and  $q$  are two indices allowing to estimate various characteristic diameters such as numerical (arithmetic) mean diameter ( $D_{10}$  with  $p=1$  and  $q=0$ ), "surface mean" diameter ( $D_{20}$  with  $p=2$  and  $q=0$ ), "volume mean" diameter ( $D_{30}$  with  $p=3$  and  $q=0$ ), and SMD ( $D_{32}$  with  $p=3$  and  $q=2$ ) so-called Sauter mean diameter.

In Table 1, it can be noted that these mean diameters decrease with an increase of the operating pressure. The Sauter diameter ( $D_{32}$ ) ranges from 226  $\mu\text{m}$  at 4 bars to 202  $\mu\text{m}$  at 8 bars. Despite the fact that the flow rate increases about 50% between 4 and 8 bars, the operating pressure has a limited effect on the droplet distribution.

Some attempts were done to identify droplet distributions thanks to a log-normal distribution based on experimental results. This droplet distribution is given as a function of the diameter  $d$  by,

$$f(d) = \frac{1}{\sqrt{2\pi}d\sigma} \exp\left(-\frac{1}{2\sigma^2} \left(\ln\left(\frac{d}{\mu}\right)\right)^2\right) \quad (3)$$

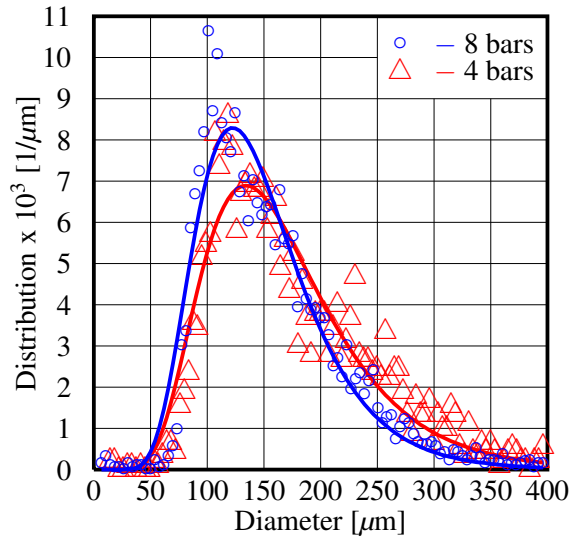


Figure 3: Comparison of the droplet distributions for TP400067 between 4 and 8 bars. Symbols stand for experimental results and solid lines are the optimized distributions

where  $\mu$  is the mean of the distribution and  $\sigma$  the standard deviation. Some complementary tests (not presented here) have been done with other droplet distributions, such as Rosin Rammler or Weibull law, but the log-normal seems to be the best compromise to represent the sprays used in this study. It is also often used in standard CFD codes applied to fire safety simulations.

A Particle Swarm Optimization [22] was used in a minimization algorithm for the parameter optimization. The characteristic parameters obtained for the two droplet distributions are given in Table 1. The comparison between the two droplet distributions can be seen in Figure 3 with a correct agreement between experimental and optimized results.

The nozzle was positioned in Zone #3 in the middle between the two thermocouple trees Row #1 and #2 as depicted in Figure 1(a). This configuration allows to study the smoke - spray interactions without impacting the fire itself. Hence, it was verified that the production of smoke remains constant during each experiment.

Figure 4 was taken from the exit of the corridor. The two thermocouple trees can be seen and the stratified layer of smoke is flowing on the upper part below the ceiling. The fire is at the left hand side of the corridor end. Here, the injection nozzle is in an upward position with an angle of 45°.

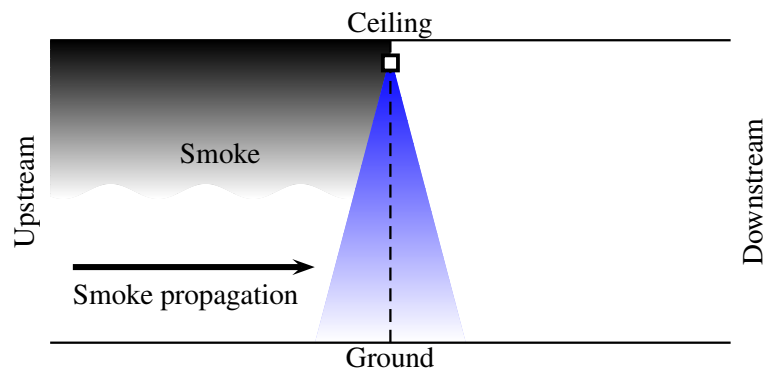


Figure 4: Rear view from the exit of an upward water spray with a 45° angle

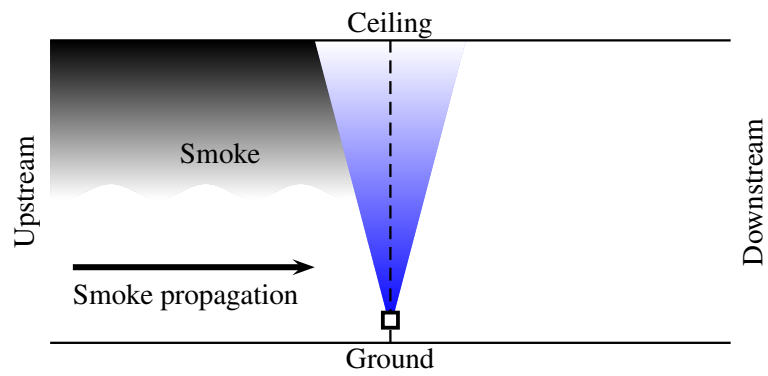
As the aim of this study is to quantify the effects of an upward water spray (either with an inclined or a vertical action) on a smoke layer, different scenarios were considered by varying the spray orientation ( $-90^\circ$ ,  $45^\circ$  or  $90^\circ$  as shown in Figure 5) and the operating pressure (4 or 8 bars). The experimental tests were repeated three times to check the result repeatability. In a nutshell, 19 experimental tests were carried out. Table 2 gives a summary of all tested parameters and the total number of repetitions for each configuration.

Test #1 was defined as a reference case without water spray. The aim was to check that the fire is not affected by the water spray activation in the other experiments. The water spray was activated when the steady state is reached in the fire development until its self-extinguishment.

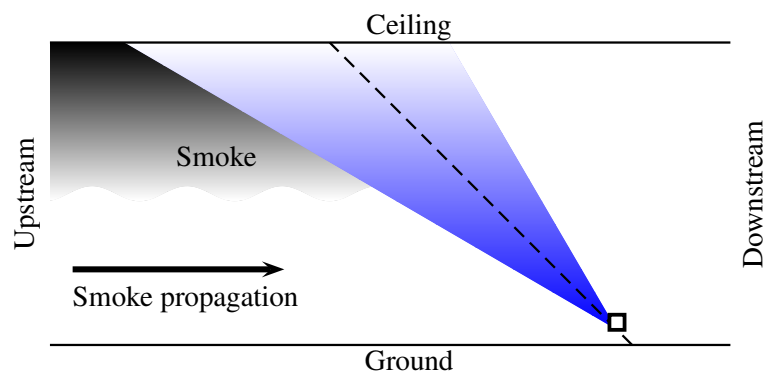
The orientation of the spray is specified for each test (vertical downward, vertical upward, inclined upward), but the exact patterns inside the corridor are not known. Indeed, it is not possible to track the distribution of droplets because the smoke fills the corridor and the opacity makes the measurement or any picture impossible. In the same way, it is not possible to quantify the water amount deposited on the walls (ceiling, ground or lateral walls) and the trajectory of droplets possibly dragged downstream by the smoke flow. Though, such phenomena were observed (water was seen on the walls after the experiments for instance) and probably influence the experimental results.



(a) Downward action (sprinkler) - Injection angle  $-90^\circ$



(b) Upward action (anti-sprinkler) - Injection angle  $+90^\circ$



(c) Inclined upward action (firefighter) - Injection angle  $+45^\circ$

Figure 5: Sketch-up (lateral views) of the three injection angles considered in this study

Test label	Injection angle	Supply pressure	Number of repetitions
[–]	[°]	[bar]	[–]
#01	Without	Without	1
#02 → #04	90	8	3
#05 → #07	45	8	3
#08 → #10	-90	8	3
#11 → #13	90	4	3
#14 → #16	45	4	3
#17 → #19	-90	4	3

Table 2: Summary of all the tested parameters and repetitions

## 2 Result analysis

### 2.1 Heat Release Rate

The first results concern the Heat Release Rate ( $HRR$ ) for each experimental configuration. Figure 6 shows the distribution of the  $HRR$  obtained during Test #1 without spray (curve in red bold). The time axis has been shifted to guarantee that  $t = 0$  s corresponds to the spray injection. For each test, the pool has been ignited 300 s before the spray activation (at  $t = -300$  s). The fire needs about 270 s to reach a steady state, where a stationary value near 28 kW can be considered. Using classical scaling laws for the present model with a geometric scale of 1/5th, the full scale heat release rate is estimated at 1.5 MW [23, 24]. After 370 s (at  $t = 70$  s), the fire extinguishes due to a lack of fuel.

In addition, the  $HRR$  profiles were plotted in Figure 6 for all tests, i.e. Test #2 to Test #19, for which the water spray is activated under different configurations of injection angles and operating pressures. All the curves follow the same trend. At the steady state, the average value of the maximum Heat Release Rate is about 28 kW with a mean standard deviation of 3 kW.

The spray is activated when the  $HRR$  reaches the steady phase after about 300 s at  $t = 0$  s in Figure 6. The spray is stopped when the fire is completely extinguished (at  $t = 70$  s). During the steady state, no significant variation is

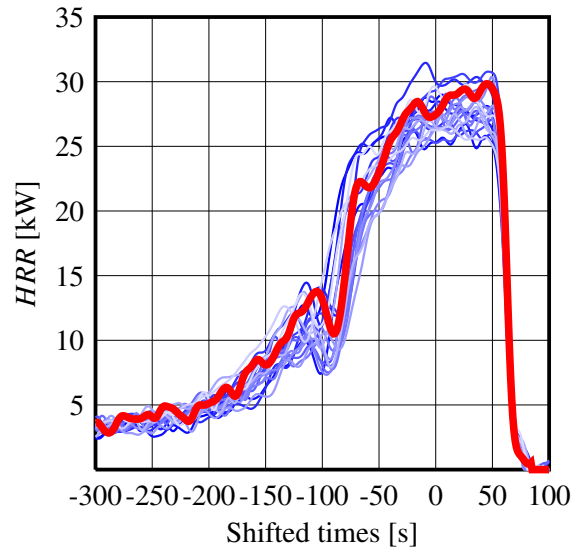


Figure 6: Heat Release Rate profiles against time for all experimental tested considered in this study. In red, the case without water spray (Test #1) and in blue, the configuration with spray activation at 300 s (from Test #2 to Test #19)

observed, demonstrating that the water spray activation has no effect on the fire development, neither on the maximal value of  $HRR$  nor on the duration of the steady state phase. Moreover, the repeatability is reasonable between each test, as it can be seen in Figure 6, with maximal discrepancies of 5 kW. If there is an effect of under-ventilation on the fire regime, it is not affected by the perturbation induced by the spray on the smoke flow in the corridor. The  $HRR$  value, beside its questionable evaluation with relationship (1), remains at least a correct approximation in all experiments.

## 2.2 Temperature data analysis for downward spray activation

Data obtained during Test #2 are used to illustrate the temperature data processing. For this test, the operating pressure is set at 8 bars and the spray is located close to the ceiling directed down to the ground ( $-90^\circ$ ). Raw data have been averaged using a 13 points sliding centered Gaussian window [25, 26] to discard any measurement noise.

Figure 7 shows the temperature profiles obtained with the thermocouple Row #1 and #2, corresponding to the trees located upstream and downstream the spray position, respectively. Each curve corresponds to a given height on the thermocouple tree. It is recalled that the distance between each thermocouple is 20 mm (the first one set at 10 mm from the floor, the second at 30 mm, . . . up to the last at 470 mm). Here again, the time axis has been shifted in order

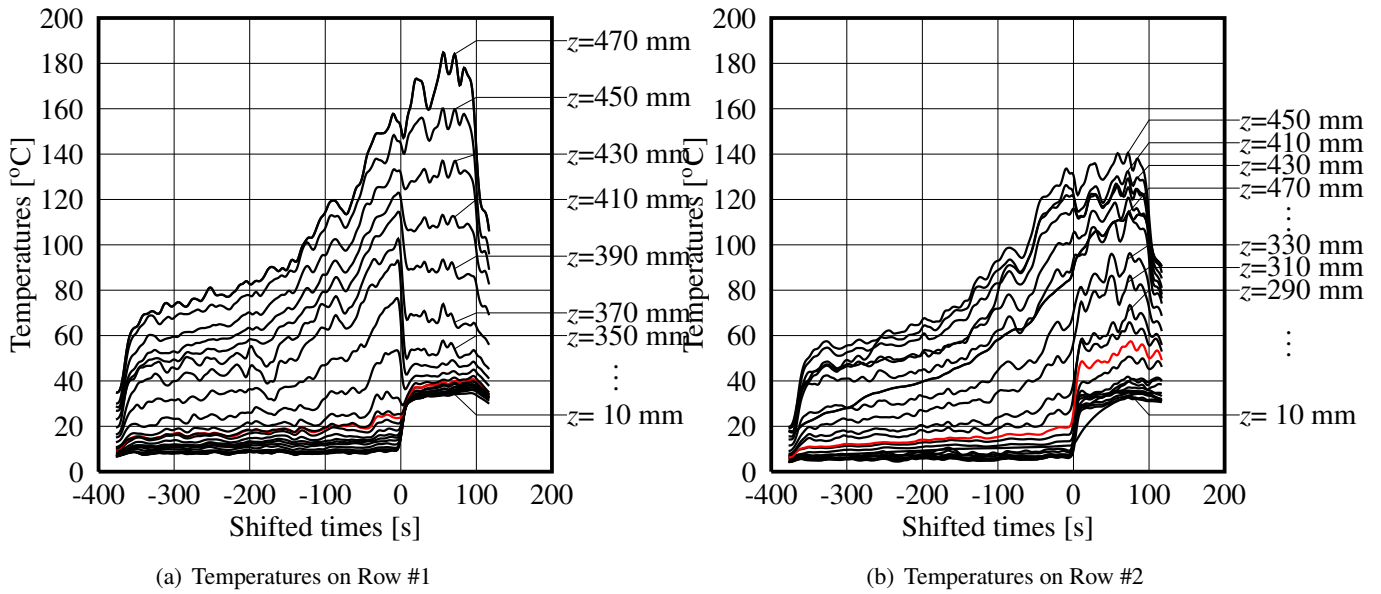


Figure 7: Temperatures on Row #1 and #2 for Test #2. The operating pressure is set at 8 bars, the nozzle is located close to the ceiling and provides a downward spray. The red curve show the temperature at mid-height in the corridor to set the activation of the water spray at 0 s.

The temperatures increase with the height, which is a common observation of smoke stratification effect. Hot smoke is flowing in the upper part of the corridor, while a cool layer is observed just above the floor (as shown by the series of curves between 0 and 20°C). Visual observations showed that this is a smoke free layer, not only a layer of cold smoke as will be observed later in some cases during the spraying action.

Once the spray is activated, a decrease of the temperature is observed in the upper part of the corridor on Row #1 (except for the three upper thermocouples, as explained afterwards), while an increase of the temperature is observed in the lower part. As the waterspray partially stops the spread of smoke, the smoke fills the space upstream the spray and a mixing is observed with the fresh air still present in the lower part. This results in a temperature increase in the lower part of the corridor with a collapse of the lowest curves indicating that a complete mixing is obtained. However, a stratification still remains in the upper part, as hot smoke continues to flow from the fire location. The three upper thermocouples even show a further increase for Row #1. This is due to the fact that the nozzle could not be set exactly at the ceiling, but with a 4 cm gap. This provides an upper layer where the smoke is flowing above the spray itself, not cooled or mixed by the spray activation. On Row #2, downstream the spray location, all temperatures are either stable

or even increasing after the spray activation, showing no cooling effect due to the spray action. This can be partly explained by the hot smoke flowing above the spray. In addition, there is no effective smoke containment, because smoke is continuously produced by the fire and flows across/rounds the water curtain. Finally, one cannot rule out a possible influence of water vapor generated by the droplets on the results (with a limited contribution however, since the residence time of droplets inside the corridor and the water flowrate are weak). In the lower part, the observed increase is also due to the smoke mixing. The red lines correspond to a mid-height vertical position, they show that the spray activation does not provide any cooling effect at this intermediate height.

Note that the temperatures do not start exactly from the same value (ambient temperature for instance) because the experimental setup has been heated by previous tests. Nevertheless, the discrepancies in the initial thermal conditions do not affect the fire development since the Heat Release Rate profile is quite the same whatever the configuration tested.

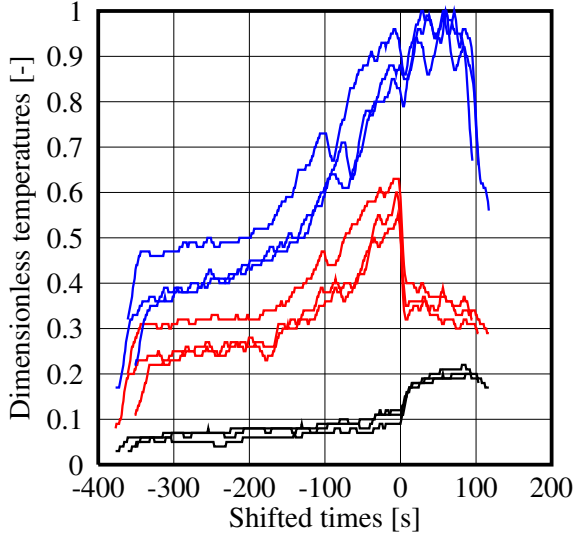
Dimensionless temperatures have been estimated to avoid the influence of the pre-heating phase and to allow a better comparison between the tests. The following ratio has been used,

$$\tilde{T} = \frac{T - T_{min}}{T_{max} - T_{min}} \quad (4)$$

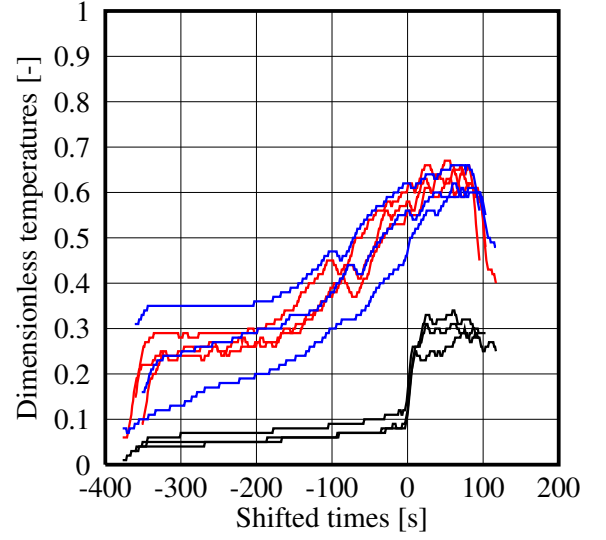
where  $T_{min}$  and  $T_{max}$  simply stand for minimum and maximum values of temperature for each individual test.

These dimensionless temperature provides values in the range between 0 and 1. Figure 8 presents the results obtained for three repeatability tests (Test #2 to Test #4). The time axis has been shifted in order to set the activation of the water spray at 0 s. The comparison is only proposed on 3 heights corresponding to  $z=230$  mm (black lines), 350 mm (red lines) and 470 mm (blue lines). The experimental data show a good repeatability, with a maximum relative discrepancy estimated at 10% for Row #1 and 20% for Row #2. The spray activation has no effect on the temperature at the highest position upstream from the injection (blue curves on Row #1), in accordance with the reason explained above (smoke can flow above the nozzle at this height). A cooling is observed downstream the nozzle, due to a strong mixing effect that reduces the smoke stratification. For the other vertical positions, the spraying action results in a temperature decrease at 350 mm (red curves) upstream from the nozzle, showing a cooling effect, while an increase is observed at mid-height (black curves) due to a strong mixing effect of the smoke on the whole height. This mixing is even more pronounced downstream the nozzle (Row #2) with all temperatures ranging in a smaller interval and since





(a) Temperatures on Row #1



(b) Temperatures on Row #2

Figure 8: Temperatures on Row #1 and #2 for Test #2 , #3 and #4. The operating pressure is set at 8 bars, the nozzle is located close to the ceiling and provides a downward spray. Blue curves are for height 470 mm, red for 350 mm and black for 230 mm

values obtained at mid-height show a further increase.

Actually, a spray with a downward injection produces a thermal destratification upstream and downstream the water spray, with only partial cooling at some heights, but a temperature increase on the contrary in the lower part of the corridor. This is due to the momentum of the water spray pushing the smoke downwards.

The vertical position of the interface between the upper layer and the lower layer can be estimated using the temperature profiles measured in the corridor. The method proposed by Quintiere *et al.* [27] and popularized by Janssens and Tran [28] has been used. In assuming that the lower layer of fresh air has a constant temperature, the thickness of the upper layer (smoke layer thickness  $H - Z_{int}$ ) is calculated by solving the following set of equations,

$$(H - Z_{int}) T_{up} + Z_{int} T_{low} = \int_0^H T(z) dz \quad (5)$$

$$\frac{(H - Z_{int})}{T_{up}} + \frac{Z_{int}}{T_{low}} = \int_0^H \frac{1}{T(z)} dz \quad (6)$$

where  $T_{up}$  is the upper layer temperature (temperature of the smoke layer),  $T_{low}$  is the lower layer temperature, which

	Before spray activation		After spray activation	
	Row #1	Row #2	Row #1	Row #2
$T_{up}$ [K]	$131.1 \pm 1.7$ °C	$97.9 \pm 1.0$ °C	$143.1 \pm 2.7$ °C ↑	$102.9 \pm 4.0$ °C ↗
$Z_{int}$ [cm]	$30.5 \pm 1.9$ cm	$25.8 \pm 1.1$ cm	$35.6 \pm 0.4$ cm ↑	$26.5 \pm 1.5$ cm ≈

Table 3: Mean values for  $Z_{int}$  and  $T_{up}$  for Test #8-#10 on Row #1 and Row #2 for a downward spray at 8 bars. The average values are computed for 5 seconds before spray activation and 30 seconds after. Symbols (arrow or approximate sign) indicate the trend observed for  $T_{up}$  or  $Z_{int}$

is assumed to be equal to the air temperature at the ground (i.e.  $T_{low} = T(z = 0)$ ),  $Z_{int}$  is the position of the interface between the smoke layer and the fresh air,  $H$  corresponds to the corridor height and  $z$  is the vertical coordinate. All the temperatures for Eq.(5) and (6) are considered in Kelvin. Care should be taken when analyzing the data in the present cases, because a strong mixing by the spray activation may result in the total lack of a smoke-free layer or in a near-linear profile of the temperature which is due to the presence of smoke over the entire height of the corridor. In this case the method originally suited for a two layer configuration (smoke / fresh air) is no more reliable. When there is a remaining thermal stratification, the value are still provided in the following sections. The evaluation of  $Z_{int}$  and  $T_{up}$  is used as an indication of a possible loss of stratification and cooling or heating of the smoke layer.

Table 3 sums up the characteristic values obtained for  $Z_{int}$  and  $T_{up}$ . A Levenberg-Marquardt algorithm was used to solve the non linear system given by Eq.(5)-(6). Data were averaged over a period of 5 seconds before spray activation and 30 seconds after, considering the three Tests #2-#4 (two choices made to ascertain stability and repeatability). The upper layer is thickened after the spray activation, both upstream and downstream the spray owing to the values obtained for  $Z_{int}$  and the temperature of the smoke layer is also increased on both positions, showing that the spraying action results in no cooling effect. Based on visual observations, the main observed effect of the spray on the smoke layer is to block their spread along the corridor.

### 3 Efficiency of different water spray actions on a smoke layer

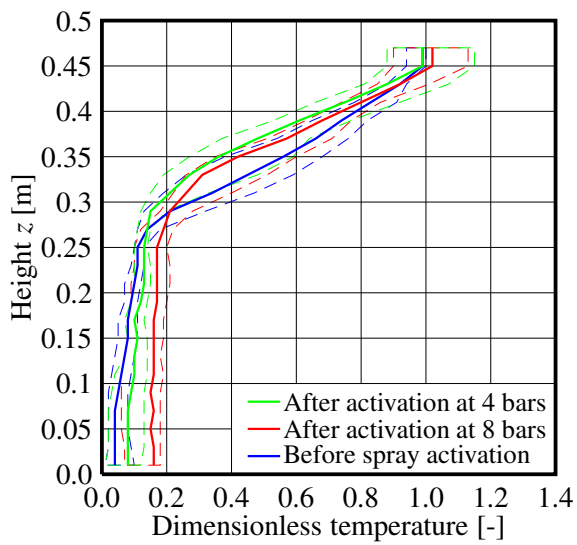
The impact of the spray activation on the smoke flow in the corridor is now compared for the three investigated angles of injection, downward (-90°), upward vertically (+90°) and upward inclined (+45°). The emphasis is put on the alteration of the thickness and the temperature of the smoke layer, expecting a cooling effect, a possible smoke containment at least partially and if possible without total loss of a smoke-free layer in the lower part of the corridor.

#### 3.1 Impact of a downward spray injection on the smoke flow

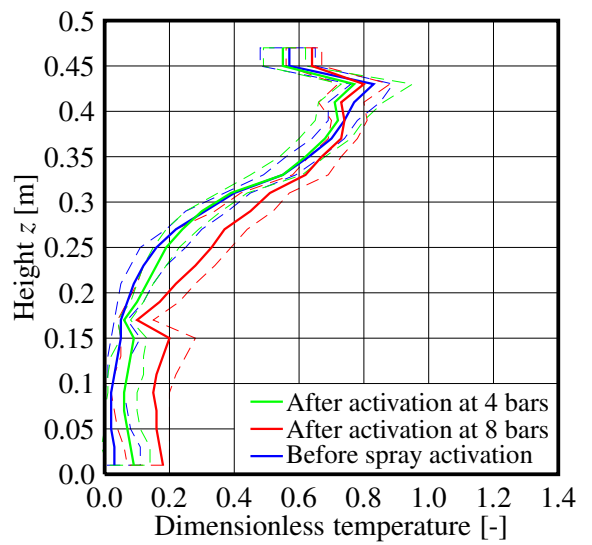
The experimental data for the temperature are non-dimensionalized by applying Eq.(4). The values are then averaged over 5 seconds before the spray activation and 30 seconds after.  $T_{min}$  and  $T_{max}$  are respectively the minimum and the maximum temperature observed on the thermocouple trees during the 5 seconds before the spray activation. Figure 9(a) and 9(b) give the temperature profiles for Row #1 and Row #2 , respectively.

As can be observed, there is an obvious smoke stratification before the spray activation (blue curve), in accordance with the results provided in Table 3. Once the spray is activated, a slight decrease of the temperature is seen in the upper part of the corridor upstream the nozzle location, while a limited alteration is seen downstream the spray. These observations hold for all repeatability tests, as shown by the dashed lines which correspond to the minimum and maximum values measured for all tests). In the lower part a temperature increase is observed, both upstream and downstream the spray, as a consequence of a mixing effect. The mixing is moderate, but yet obvious, resulting in a slight increase of the smoke layer thickness. A stratification is still observed if temperatures are the only investigated data, but the presence of cold smoke is possible in the lower part. Actually, the spray has only a limited impact on the smoke flow and has no positive expected effect like smoke cooling or containment.

As two pressures (4 and 8 bars) were used during the experiments, one can observe that there is an effect of the water supply, with an enhanced impact on the upper layer of the spray for the highest pressure, which is logical as it results in a higher flow rate and a smaller size distribution, both expected to increase momentum and heat exchanges.

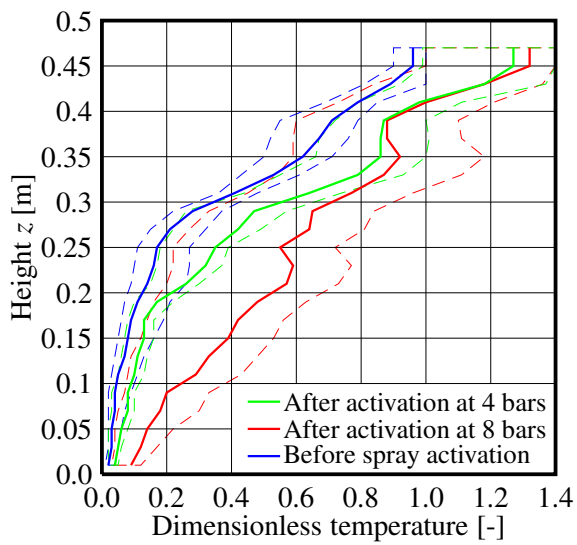


(a) Temperature profiles at Row #1 - Upstream

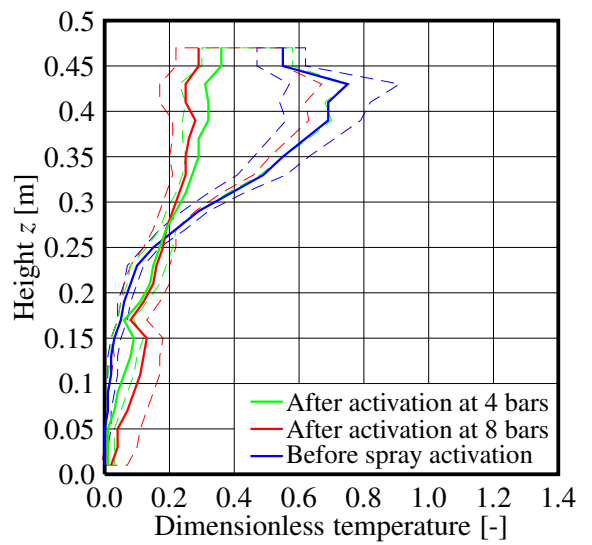


(b) Temperature profiles at Row #2 - Downstream

Figure 9: Results on the mean temperature profiles (average on 5 seconds before spray activation, in solid blue lines, and on 30 seconds after, in solid red or green lines) for a downward action. The solid lines are the mean profiles and the dashed lines correspond to the maximum and minimum values. Tests on two operating pressures 4 and 8 bars



(a) Temperature profiles at Row #1 - Upstream



(b) Temperature profiles at Row #2 - Downstream

Figure 10: Results on the mean temperature profiles (average on 5 seconds before spray activation, in solid blue lines, and on 30 seconds after, in solid red or green lines) for a vertical upward action. The solid lines are the mean profiles and the dashed lines correspond to the maximum and minimum values. Tests on two operating pressures 4 and 8 bars

	Before spray activation		After spray activation	
	Row #1	Row #2	Row #1	Row #2
$T_{up}$ [K]	$125.6 \pm 4.4$ °C	$97.9 \pm 1.0$ °C	$161.2 \pm 9.8$ °C ↑	$88.7 \pm 3.3$ °C ↘
$Z_{int}$ [cm]	$27.1 \pm 0.7$ cm	$23.9 \pm 0.8$ cm	$18.6 \pm 0.8$ cm ↘	$17.9 \pm 2.2$ cm ↘

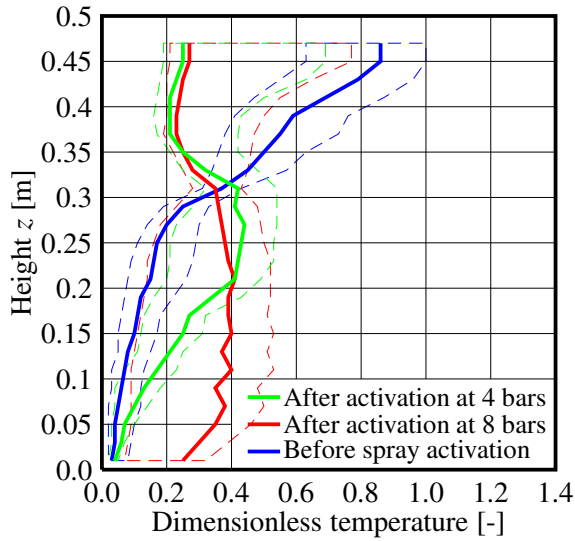
Table 4: Mean values for  $Z_{int}$  and  $T_{up}$  for Test #2-#4 on Row #1 and Row #2 for vertical upward injection at 8 bars. The average values are computed for 5 seconds before spray activation and 30 seconds after. Symbols (arrow or approximate sign) indicate the trend observed for  $T_{up}$  or  $Z_{int}$

### 3.2 Vertical upward injection

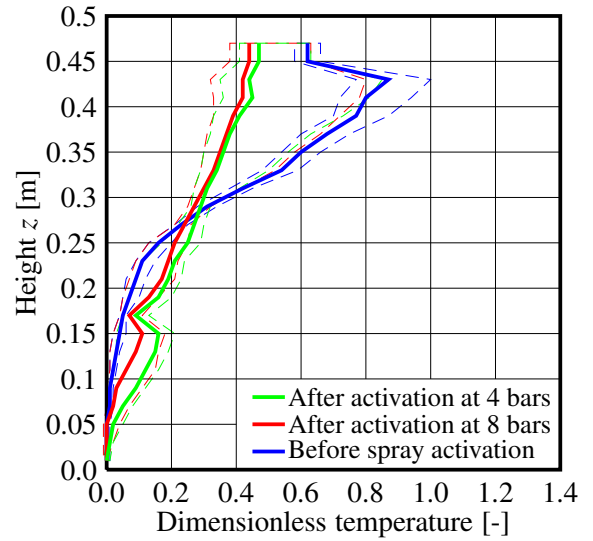
The same analysis is now conducted for a spray activation with an upward vertical injection (+90°). Results are presented in Figure 10, still provided for the two operating pressures 4 and 8 bars, and compared with the situation before the spraying action. These profiles correspond to the averages of three tests: Test #8 to #10 for 8 bars, Test #17 to #19 for 4 bars. Of course the profiles given before the spray activation show the same stratification as previously commented in Figure 9.

Due to the upward injection, droplets are supposed to interact with the smoke flow for a longer time, with an ascending phase until a complete deceleration and a descending phase with a null initial velocity, also possibly dragged longitudinally by the smoke flow. In consequence, the residence time of droplets inside the corridor increases.

Figure 10(a) (upstream from the nozzle location) shows that a temperature stratification is kept after the spray activation, but an obvious mixing results in the loss of the smoke-free layer. The temperature increases in the whole first part of the corridor, due to a containment effect of the smoke, which is not totally blocking the smoke but still induces a partial containment. The above-described enhanced momentum exchange due to the particular trajectories of the droplets has a clear impact on the profiles. Downstream the nozzle (see Figure 10(b)), a cooling of the upper layer of the smoke is observed, while a slight increase is seen in the lower part as a consequence of the mixing effect. This effect is enhanced with an increased water supply upstream from the spray, but to a lesser extent downstream from the spray.



(a) Temperature profiles at Row #1 - Upstream



(b) Temperature profiles at Row #2 - Downstream

Figure 11: Results on the mean temperature profiles (average on 5 seconds before spray activation, in solid blue lines, and on 30 seconds after, in solid red or green lines) for an inclined upward action. The solid lines are the mean profiles and the dashed lines correspond to the maximum and minimum values. Tests on two operating pressures 4 and 8 bars.

Table 4 sums up the characteristic values obtained for  $Z_{int}$  and  $T_{up}$  for vertical upward injection at 8 bars. The hot smoke layer is thinner, both upstream and downstream the spray regarding the values performed for  $Z_{int}$ . It should be reminded here, that the evaluation is based on the temperature profiles, as an indication of thermal stratification. These profiles are near linear indicating that colder smoke mixed with air is present in the bottom part. The smoke-free layer is no more observed. The temperature of the smoke layer, upstream the spray, increases demonstrating again that the smoke is contained. Downstream the spray, the temperature decreases thanks to both cooling and evaporating effects from droplets, since their lifetimes inside the corridor have increased.

For the fire safety concerns, this spray action allows to contain the smoke propagation, with a cooling effect of the upper smoke layer in addition. The lower part still keeps acceptable conditions regarding the thermal stresses at least.

### 3.3 Inclined upward action at 45°: firefighter mode

The results obtained for an inclined upward action at 45°, such as a nozzle activation during firefighting operations, are presented in Figure 11 with the same operating pressures 4 and 8 bars. Each profile corresponds to an average of

	Before spray activation		After spray activation	
	Row #1	Row #2	Row #1	Row #2
$T_{up}$ [K]	$125.6 \pm 4.4$ °C	$97.9 \pm 1.0$ °C	-	$88.7 \pm 3.3$ °C ↘
$Z_{int}$ [cm]	$30.4 \pm 1.5$ cm	$24.3 \pm 0.6$ cm	-	$19.0 \pm 1.7$ cm ↘

Table 5: Mean values for  $Z_{int}$  and  $T_{up}$  for Test #5-#7 on Row #1 and Row #2 for inclined upward action at 45° at 8 bars. The average values are computed for 5 seconds before spray activation and 30 seconds after. Values obtained for Row #1 are non physical because no clear stratification is observed, results are not provided. Symbols (arrow or approximate sign) indicate the trend observed for  $T_{up}$  or  $Z_{int}$

three tests: Test #5 to #7 for 8 bars, Test #14 to #18 for 4 bars.

With this configuration, reversed temperature profiles are observed on the tree located upstream from the spray, i.e. the lower part of the corridor becomes warmer than the upper part for both operating pressures and with an enhanced effect for the higher pressure. The loss of stratification is complete. The spray strongly impacts the upper layer resulting in an effective cooling effect, but the mixing is so strong that smoke fills the whole corridor. The expected containment effect is obtained, but the environment upstream the spray is highly impacted by the smoke over the entire height. Downstream the nozzle location, there is a remaining stratification, at least considering the temperature profiles (cold smoke might be present and penalizes the visibility).

The cooling effect is clearly visible, in particular for the upper part of the corridor. Indeed, in comparison with the case of a vertical upward injection, the spray effect is enhanced upstream from the nozzle with a stronger containment effect and a similar impact is measured downstream the nozzle with a cooling effect but also a mixing which affects the lower part of the corridor.

Table 5 gives the characteristic values obtained for  $Z_{int}$  and  $T_{up}$  for inclined upward injection at 8 bars. The results for Row #1 are not provided since the lack of thermal stratification on the temperature profile does not allow to calculate reliable results. Nevertheless, downstream the spray, one can observe a decrease both on the smoke layer thickness and on the temperature. This kind of action promotes the cooling and containing effects on the smoke by the droplets.



The impact of the inclined upward action is the most efficient, with the strongest cooling effect that could help to avoid the occurrence of thermal hazards, such as a smoke ignition for instance. This could be seen as a help for firefighters to move forward in the corridor for instance.

## 4 Conclusion and further works

Experiments were conducted in a reduced scale model ( $1/5^{th}$ ) to study the smoke/spray interactions in a corridor when a spray is activated in a stratified smoke flow. The setup was built in order to promote an impact on the smoke, while preserving the fire itself, so that the smoke production remains unchanged. These tests were intended to observe cooling, containment and mixing effects on the smoke flow when the spray is activated downward, upward vertically or with a  $45^\circ$  angle in a counter-flow.

The tests showed that this inclined injection at  $45^\circ$  provides the most efficient cooling and containment effects upstream and downstream the nozzle location. An obvious cooling is obtained in the upper part while causing limited heating in the lower part, in particular downstream from the spray, at least in the configuration of the experimental setup studied (with a 4 or 8 bars operating pressure). In addition, this type of injection was observed to preserve a cold layer in the lower part, i.e. in the area where the firefighters are present when progressing in a corridor in the direction of the fire. This stronger impact by the droplets can be easily explained by an enhanced residence time of the droplets in the smoke flow and a counter-flow impact, both contributing to increase the heat and momentum exchanges, in particular. The drawback is a loss of stratification upstream from the spray location due to stronger containment and mixing effects.

The upward vertical injection provides similar temperature conditions downstream the spray, but the containment of smoke is less obvious and the cooling effect is not observed in the upper layer of the smoke upstream the spray.

The least efficient impact is observed for the downward vertical injection, as a consequence of a limited residence time and a quick deposit of droplets on the floor penalizing the heat and momentum exchanges with the smoke flow, compared to the other injection solutions. This action has a weak impact on the smoke flow and does not improve the environment considering safety concerns for firefighters, for instance.

It should be noted that these experiments do not take into account other important parameters for firefighters: water

injected by pulses instead of continuous water application, production of water vapor, the possible consequences on them (thermal injuries), the radiation received near the floor . . . Hence, conclusions should be taken with care before further study or extrapolation to the real scale. Moreover, for further works, a special attention should be paid to analyze the spray application on the smoke opacity.

The tests also show that the supply pressure has an influence on the global mixing and cooling phenomena, which was limited in the present tests because one single nozzle was used and since the droplet size distribution in particular was only weakly altered by the change in feeding pressure.

In addition, this study will be supplemented by numerical simulations, with specific mass and energy balances to estimate the importance of the various heat, momentum and mass transfer phenomena involved in the smoke/spray interactions.

Finally, further tests could be also conducted to investigate the effect of a small amount of additive in waterspray on the smoke control or on the fire extinguishing. Foam or wetting agents are commonly used by the firefighters and can have a significant impact on their fire safety.

## **Declarations**

**Conflict of interest.** The authors declare that they have no known competing financial or non-financial interests or personal relationships that could have appeared to influence the work reported in this paper.

## **Data availability**

All the experimental data used in the frame of this study are available in the open database DOREL (DONnées de REcherche Lorraines) [29]. For each Test, 2 files are proposed: the first contains all the temperatures profiles against time ; the second gives the mass loss as a function of time. The spray activation is defined at  $t = 0$  s. Two supplementary files have been added containing the recordings (droplet diameters and velocities) for the spray distributions used in this work: TP 400067 at 4 and 8 bars.

## References

- [1] J. Sun, Z. Fang, Z. Tang, T. Beji and B. Merci. Experimental study of the effectiveness of a water system in blocking fire-induced smoke and heat in reduced-scale tunnel tests. *Tunnelling and Underground Space Technology*, 55:34–44, 2016.
- [2] R. Mehaddi, A. Collin, P. Boulet, Z. Acem, J. Telassamou, S. Becker, F. Demeurie and J.-Y. Morel. Use of a water mist for smoke confinement and radiation shielding in case of fire during tunnel construction. *International Journal of Thermal Sciences*, 148:106156, 2020.
- [3] G. Parent, P. Boulet, S. Gauthier, J. Blaise and A. Collin. Experimental investigation of radiation transmission through a water spray. *Journal of Quantitative Spectroscopy and Radiative Transfer*, 97(1):126–141, 2006.
- [4] A. Collin, P. Boulet, G. Parent and D. Lacroix. Numerical simulation of a water spray - Radiation attenuation related to spray dynamics. *International Journal of Thermal Sciences*, 46(9):856–868, 2007.
- [5] M.L. Bullen. The effect of a sprinkler on the stability of a smoke layer beneath a ceiling. *Fire Technology*, 13:21–34, 1977.
- [6] L.Y. Cooper. The interaction of an isolated sprinkler spray and a two-layer compartment fire environment. *International Journal of Heat and Mass Transfer*, 38(4):679–690, 1995.
- [7] Y.F. Li and W.K. Chow. Study of water droplet behavior in hot air layer in fire extinguishment. *Fire Technology*, 44(4):351–381, 2008.
- [8] K.Y. Li and M.J. Spearpoint. Simplified calculation method for determining smoke downdrag due to a sprinkler spray. *Fire Technology*, 47(3):781–800, 2010.
- [9] Z. Tang, Z. Fang, J.P. Yuan and B. Merci. Experimental study of the downward displacement of fire-induced smoke by water sprays. *Fire Safety Journal*, 55:35–49, 2013.
- [10] Z. Tang, J. Vierendeels, Z. Fang and B. Merci. Description and application of an analytical model to quantify downward smoke displacement caused by a water spray. *Fire Safety Journal*, 55:50–60, 2013.

- [11] Z. Tang, Z. Fang and B. Merci. Development of an analytical model to quantify downward smoke displacement caused by a water spray for zone model simulations. *Fire Safety Journal*, 63:89–100, 2014.
- [12] R. Morlon, P. Boulet, G. Parent, S. Lechêne, E. Blanchard, C. Rebuffat, P. Fromy, J.-P. Vantelon and D. Borgiallo. Study of de-stratification and optical effects observed during smoke/mist interactions. *Fire Technology*, 51(5):1231–1248, 2015.
- [13] E. Blanchard, R. Morlon, G. Parent, P. Fromy, P. Boulet and D. Borgiallo. Experimental study of the interaction between water sprays and smoke layer. *Fire Technology*, 54(2):479–501, 2018.
- [14] R. Mehaddi, P. Laboureur, A. Braconnier, P. Boulet, S. Haouari-Harrak, A. Collin, S. Becker and J.-Y. Morel. Experimental characterization of a smoke flow in a small length corridor. *Fire Technology*, 56(2):883–889, 2020.
- [15] M.J. Hurley, D. Gottuk, J.R. Hall, K. Harada, E. Kuligowski, M. Puchovsky, J. Torero, J.M. Watts and C. Wieczorek. *SFPE Handbook of fire protection engineering*, Volume 1. Springer, 2015.
- [16] S. Lechêne, Z. Acem, G. Parent, G. Jeandel and P. Boulet. Upward vs downward injection of droplets for the optimization of a radiative shield. *International Journal of Heat and Mass Transfer*, 54(9-10):1689–1697, 2011.
- [17] S. Lechêne, Z. Acem, G. Parent, A. Collin and P. Boulet. Radiative shielding by water mist: comparisons between downward, upward and impacting injection of droplets. *Journal of Physics: Conference Series*, 369:012027, 2012.
- [18] E. Roumpea, N.M. Kovalchuk, M. Chinaud, E. Nowak, M. J. Simmons and P. Angeli. Experimental studies on droplet formation in a flow-focusing microchannel in the presence of surfactants. *Chemical Engineering Science*, 195:507-518, 2019.
- [19] I. Kiratzis, N.M. Kovalchuk, M. J. Simmons and D. Vigolo. Effect of surfactant addition and viscosity of the continuous phase on flow fields and kinetics of drop formation in a flow-focusing microfluidic device. *Chemical Engineering Science*, 248:117183, 2022.
- [20] W. Schäfer and C. Tropea. The time-shift technique for measurement of size and velocity of particles. ILASS - Europe 2011, 24th European Conference on Liquid Atomization and Spray Systems, Estoril, Portugal, 2011.

- [21] W. Schäfer, C. Tropea, G. Wigger and D. Eierhoff. Spray measurements with the time-shift technique. *Measurement Science and Technology*, 32(10):105202, 2021.
- [22] J. Kennedy and R. Eberhart. Particle Swarm Optimization Proceedings of the IEEE International Conference on Neural Networks, 4:1942–1948, IEEE Press, 1995.
- [23] J.G. Quintiere. Scaling applications in fire research. *Fire Safety Journal*, 15(1):3–29, 1989.
- [24] H. Ingason and Y.Z. Li. Model scale tunnel fire tests with longitudinal ventilation. *Fire Safety Journal*, 45(6):371–384, 2010.
- [25] A.V. Oppenheim, R.W. Schafer and J.R. Buck. Discrete-Time Signal Processing. Upper Saddle River, NJ: Prentice Hall, 1999.
- [26] E.W. Hansen. Fourier Transforms: Principles and Applications. New York: John Wiley & Sons, 2014.
- [27] J.G. Quintiere, K. Steckler and D. Corley. An assessment of fire induced flows in compartments. *Fire Science and Technology*, 4 (1):1–14, 1984.
- [28] M. Janssens and H.C. Tran. Data reduction of room tests for zone model validation. *Journal of Fire Sciences*, 10 (6):528–555, 1992.
- [29] A. Collin, L. Hardy, M. Suzanne, G. Erez, R. Mehaddi and P. Boulet. Experimental data on the interaction between a water spray and a moving layer of hot smoke. <https://doi.org/10.12763/U1JZNG>, Université de Lorraine, 2023.